

# Influence of copper on the electronic properties of amorphous chalcogenides

S. I. Simdyankin,<sup>1,\*</sup> M. Elstner,<sup>2,3</sup> T. A. Niehaus,<sup>2,3</sup> Th. Frauenheim,<sup>3</sup> and S. R. Elliott<sup>1</sup>

<sup>1</sup>*Department of Chemistry, University of Cambridge,  
Lensfield Road, Cambridge CB2 1EW, United Kingdom*

<sup>2</sup>*German Cancer Research Center, Dept. Molecular Biophysics, D-69120 Heidelberg, Germany*

<sup>3</sup>*Fachbereich 6 — Theoretische Physik, Universität Paderborn,  
Warburger Straße 100, D-33098, Paderborn, Germany*

(Dated: November 9, 2018)

We have studied the influence of alloying copper with amorphous arsenic sulfide on the electronic properties of this material. In our computer-generated models, copper is found in two-fold near-linear and four-fold square-planar configurations, which apparently correspond to Cu(I) and Cu(II) oxidation states. The number of overcoordinated atoms, both arsenic and sulfur, grows with increasing concentration of copper. Overcoordinated sulfur is found in trigonal planar configuration, and overcoordinated (four-fold) arsenic is in tetrahedral configuration. Addition of copper suppresses the localization of lone-pair electrons on chalcogen atoms, and localized states at the top of the valence band are due to Cu  $3d$  orbitals. Evidently, these additional Cu states, which are positioned at the same energies as the states due to  $[\text{As}_4]^-$ - $[\text{S}_3]^+$  pairs, are responsible for masking photodarkening in Cu chalcogenides.

PACS numbers: 71.23.Cq, 61.43.Dq,

There has been a significant amount of experimental research on the role of copper in amorphous chalcogenide alloys. It is generally believed that copper is found in tetrahedral configuration and is bonded exclusively to chalcogen atoms [1, 2]. However, as noted in Ref. [1], the interpretation of experimental radial distributions of ternary systems is necessarily ambiguous. More recent experimental results [3] indicate that copper also bonds to arsenic as well as to chalcogen atoms. It was observed [4] that photodarkening (red shift of the optical absorption edge under illumination) disappears in  $\text{Cu}_x(\text{As}_{0.4}\text{Z}_{0.6})_{1-x}$  alloys, starting from  $x = 1\%$  for  $\text{Z}=\text{S}$  and  $x = 5\%$  for  $\text{Z}=\text{Se}$ . Two possible interpretations of this observation, given in Ref. [5], are either that the photodarkening is masked by some electronic states due to Cu atoms, or the addition of copper interferes with correlations of lone-pair orbitals on a scale greater than that of a nearest-neighbor distance. Alternatively, the Cu-related states at the band edges may be efficient non-radiative centers which provide an alternative channel to that resulting in photostructural bond rearrangement of the chalcogenide network. The observation that photoinduced phenomena, other than photodarkening, remain intact after the addition of copper [6] favors the first interpretation.

It is a natural next step in the investigation of these materials to obtain the first detailed description of their electronic and structural properties by means of computer simulation. This is the topic of this paper.

Following Refs. [7, 8], we have employed a density-functional-based tight-binding (DFTB) method [9, 10], which has allowed us to create realistic models of arsenic sulfide ( $\text{As}_2\text{S}_3$ ). The DFTB method allows one to improve upon the standard tight-binding approximation by including a so-called self-consistent charge (SCC) correc-

tion [11], derived from density-functional theory (DFT), to the total energy. The procedure for generating the tabulated data sets for pairwise interatomic interactions is outlined in Ref. [12]. The S-S [12], As-As and As-S [13], and Cu-Cu, Cu-S and Cu-As [14] tables, and information on their creation, are available from the authors. The following electron orbitals were included in the basis set:  $3s$ ,  $3p$ , and  $3d$  for S atoms;  $4s$ ,  $4p$ , and  $4d$  for As atoms; and  $3d$ ,  $4s$ , and  $4p$  for Cu atoms. Using the  $d$  orbitals, in addition to the valence  $s$  and  $p$  orbitals on the S and As atoms, has proved to be crucial to describe hypervalent compounds [12] and defect centers [7, 15].

In the description of defects and impurities in crystalline materials, an ideal crystal is the obvious reference system. The situation is more complex with amorphous solids, where no atomic configuration is unique. It is, however, still possible to use a stoichiometric (all-heteropolar) structural model as a useful reference for a binary amorphous compound. In this way, any deviation from the reference-system topology and chemical order can be considered as a defect, in direct analogy with the case of a crystal. Here, we use a stoichiometric 200-atom model of amorphous (a-) $\text{As}_2\text{S}_3$  from Ref. [8], reoptimized with a richer basis set, with  $d$  orbitals added to the As atoms. This model will be referred to as model 0, in the following.

The other models, described in the following, have been prepared by adding one (model 1, 1.6% Cu), two (model 2, 3.2% Cu), and four (model 3, 6.3% Cu) copper atoms to a 60-atom (24 As and 36 S) all-heteropolar model of a- $\text{As}_2\text{S}_3$  [7]. As we performed spin-unpolarized calculations, the identity of one S atom in model 1 was changed to As, in order to keep the total number of electrons in the model to be even. The mass densities (volumes per atom) of models 1, 2, and 3 are 3.282, 3.304,

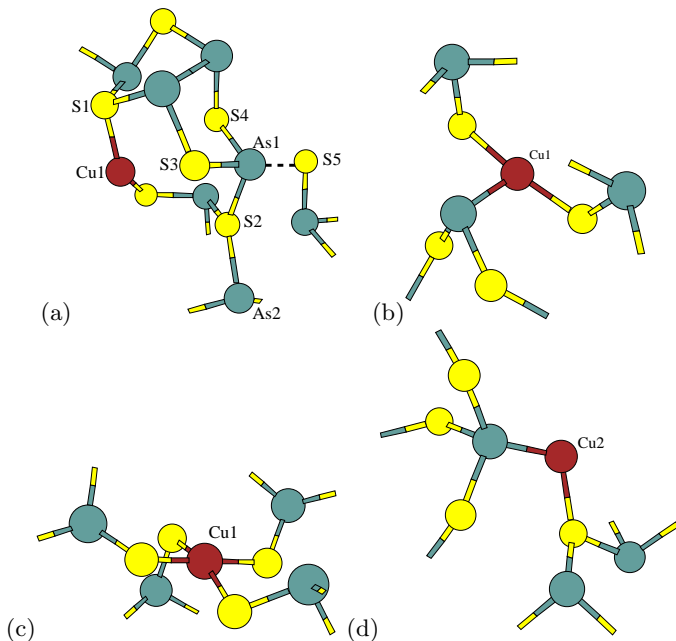


FIG. 1: Fragments of models 1 (a), 3 (b), and 2 (c,d) containing copper atoms. The dangling bonds show where the displayed configurations connect to the rest (not shown) of the network. Note that the fragments in (c) and (d) are from the same model, but they do not contain common atoms and are shown with independent and arbitrary orientations. The numbering of Cu atoms corresponds to Table I. (Color online.)

and  $3.226 \text{ g/cm}^3$  (25.371, 24.962, and  $25.791 \text{ \AA}^3/\text{atom}$ ), respectively. Keeping in mind possible local-density fluctuations in bulk amorphous alloys, by slightly varying the density of the models, we verified that the results are not particularly sensitive to this parameter for the above changes in the volume per atom. The configurations of the models used for subsequent analysis were prepared by following the melt-and-cool schedule described in Ref. [8]. Models 1, 2, and 3 correspond to energy-minimized snapshots of  $T = 300\text{K}$  configurations, and model 3a corresponds to an energy-minimized snapshot of a  $T = 700\text{K}$  configuration, where all four copper atoms were two-fold coordinated.

Fig. 1 shows copper-containing fragments of models 1, 2, and 3. These fragments illustrate typical structural motifs of the immediate environments of the Cu atoms. As seen in Table I, the coordination numbers of the Cu atoms strongly correlate with the atomic charges, which indicates the covalent nature of the bonding. The ratio of the Mulliken charges (as defined in, e.g., Ref. [8]) of four- and two-fold coordinated Cu atoms is about two, which suggests, along with the very nearly planar geometry of the four-fold coordinated Cu atom in Fig. 1(c), that such atoms are in (II) and (I) oxidation states [16], respectively. Three-fold coordinated Cu atoms (Fig. 1(b)) may be viewed as defective Cu(II) centers, also due to their

TABLE I: Coordination numbers and Mulliken charges (in atomic units) of copper atoms.

Model	Number of Cu atom	Coordination number	Mulliken charge
1	1	2	0.362
2	1	4	1.050
	2	2	0.503
3	1	3	0.826
	2	3	0.805
	3	2	0.360
	4	2	0.426
3a	1	2	0.400
	2	2	0.414
	3	2	0.420
	4	2	0.362

nearly planar geometry and reduced symmetry — the bond angles are approximately  $90^\circ$ ,  $90^\circ$ , and  $180^\circ$ .

Although the majority of Cu bonds are with S atoms (with a typical bond length  $2.3\text{-}2.4 \text{ \AA}$ ), some Cu-As bonds (with lengths of about  $2.3 \text{ \AA}$ ) are also present in the models. Invariably, one or both neighbors of the two-fold coordinated Cu(I) atoms were found to be overcoordinated (three-fold coordinated S, e.g. S1 in Fig. 1(a), or four-fold coordinated As, see Fig. 1(d)), while the bonds of Cu(II) atoms are with normally coordinated two-fold S and three-fold As atoms.

Fig. 2 shows the electronic densities of states (EDOS) and inverse participation ratios (IPR) for models 0, 2, and 3a. Mathematical definitions of both quantities, along with their local (projected) variants, are given, e.g., in Ref. [8]. The IPRs are normalized so that they are equal to unity for a totally delocalized state (equally shared by all atoms) and to  $N$ , the number of atoms in the model, for a state localized on only one atom. The most obvious distinction between the EDOS's of models 0 and 3a is the difference in the optical band gaps — the half-maximum gaps of models 0 and 3a are  $1.95 \text{ eV}$  and  $1.34 \text{ eV}$ , respectively, which accounts for the difference in the optical band gaps of pure and copper-containing  $a\text{-As}_2\text{S}_3$  observed experimentally [3, 5]. Inspection of the local EDOS (LEDOS) reveals that the main effect of the addition of copper is to modify the top of the valence band. One can say that the states due to sulfur lone-pair  $p$  orbitals are pushed down in energy, and the top of the valence band is now formed by highly localized Cu  $d$  orbitals. Copper atoms with any coordination contribute to the valence-band states, while only three- and four-fold coordinated copper atoms produce additional states at the bottom of the conduction band, as shown by the dotted line in Fig. 2(a) and solid squares in Fig. 2(b).

The above results show that the size of the optical band gap is determined by the Cu atoms in copper-containing

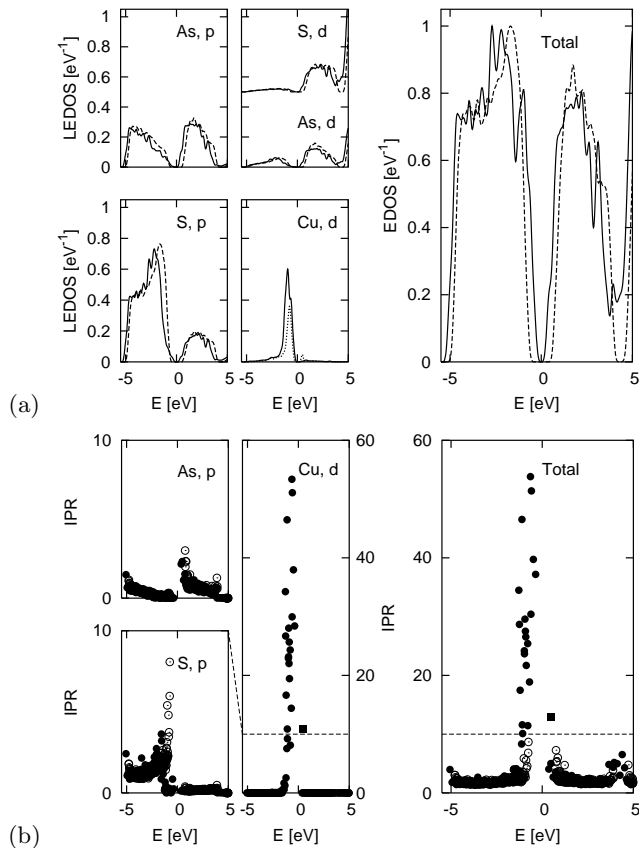


FIG. 2: (a) Total and local EDOS for models 0 (dashed line) and 3a (solid line) near the optical gap ( $E = 0$ ). The LEDOS for S,  $d$  is shifted upwards by 0.5. The dotted line in the “Cu,  $d$ ” panel corresponds to model 2. (b) Total and projected inverse participation ratios for models 0 ( $\odot$ ) and 3 ( $\bullet$ ). The dashed lines emphasize that the vertical scales of the “As and S,  $p$ ” and “Cu,  $d$ ” and “Total” axes are different. The symbol ( $\blacksquare$ ) in the “Cu,  $d$ ” and “Total” panels corresponds to model 2.

$a$ -As<sub>2</sub>S<sub>3</sub>. The Cu electronic states will mix with and mask any states due to native or photoinduced defects in the amorphous network of As and S atoms positioned at the same energies. At low Cu concentration, a significant fraction of the volume in the material is occupied by a copper-free As-S network, which should react to light in the same way as would a pure binary alloy, as suggested by experimental results [6]. It can be seen in Fig. 2(b) that, although the S  $p$  states are located deeper in the valence band because of the Cu states, they are still somewhat localized and qualitatively the localization character of S and As  $p$  states is preserved after addition of copper — the closer S  $p$  (As  $p$ ) states are to the top of the valence (bottom of the conduction) band, the more localized they are. Near-band-gap photoexcitations in this material can then be viewed as charge transfers from the normally electronegative S atoms, where the state from which an electron has been removed is predominantly localized, to the normally electropositive As atoms, where

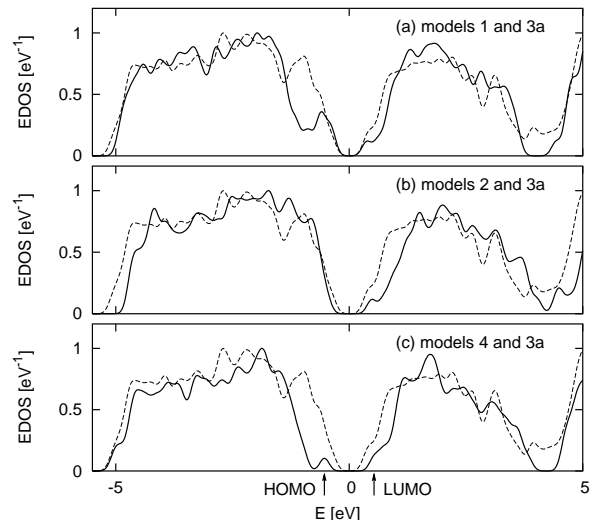


FIG. 3: EDOS near the optical gap for models 1 (a), 2 (b), and 4 (c) (solid lines). The dashed line in all panels is the same and corresponds to model 3a (same as the solid line in Fig. 2(a)). Arrows mark the HOMO and LUMO energies in model 4.

the state to which the photoexcited electron has been added is predominantly localized.

It has been shown in Ref. [7] that the excess of negative and positive charge in the vicinity of electropositive As and electronegative S atoms, respectively, produced by a photoexcitation can lead to the formation of hypervalent  $[\text{As}_4]^-$ - $[\text{S}_3]^+$  defect pairs as an alternative to radiative recombination of the photoinduced electron-hole pairs. Fig. 3(a,b) shows how the EDOS changes in the optical band-gap region in the Cu-containing models with different copper contents, while Fig. 3(c) compares the EDOS of copper-free model 4 (same as model 2(III) in Ref. [7]), containing an  $[\text{As}_4]^-$ - $[\text{S}_3]^+$  pair, with the EDOS of model 3a. The highest occupied (HOMO) state in model 4 is localized along the chain of three atoms forming the crossbar of the seesaw-like  $[\text{As}_4]^-$  center, similar to the S3-As1-S5 chain in Fig. 1(a), and the lowest unoccupied (LUMO) state is localized along an As-S bond, similar to the As2-S2 bond in Fig. 1(a), where the S atom is an  $[\text{S}_3]^+$  center. The energies of these HOMO and LUMO states are marked in Fig. 3(c), where it is seen that they are approximately equal to the energies of the Cu-related states in Fig. 3(a) and (b). The HOMO and LUMO energies in other models containing  $[\text{As}_4]^-$ - $[\text{S}_3]^+$  pairs are very close to those in model 4.

In model 1, the IPR of the LUMO state at the bottom of the conduction band is largest in the region near the  $[\text{S}_3]^+$  center (marked S2 in Fig. 1(a)), and the IPR of the seventh state counting from the top of the valence band (HOMO-7) is highest for the singly-coordinated sulfur atom (S5 in Fig. 1(a)). In this respect, the HOMO-7 state is similar to the HOMO state of copper-free models.

Promoting one electron from HOMO-7 to LUMO exerts forces on the local configuration shown in Fig. 1(a) which tend to reduce the distance between the atoms As1 and S5 (3.02 Å in the ground state) and elongate the bond S2-As2, precisely as in our time-dependent DFTB calculations on a cluster containing an  $[\text{As}_4]^-$ - $[\text{S}_3]^+$  pair in Ref. [7]. Thus the As1,S2-5 group of atoms can be viewed as a precursor of a seesaw-like  $[\text{As}_4]^-$  center, and its presence provides a channel for electron-phonon coupling that is expected to be large in these materials [17].

In summary, we have demonstrated that the main influence of small concentrations of copper on the electronic structure and optical properties of amorphous arsenic sulfide is to reduce the size of the optical band gap. The photoinduced reduction of the size of the optical band gap in pure arsenic chalcogenides, known as photodarkening, is of a similar magnitude and is not expected to be discerned in the background of Cu-state-related electronic photoexcitations. This is true even for the lowest Cu concentration, i.e. 1.6% (c.f. 1% [4]). It is noted that Cu atoms are observed in typical Cu(I) and Cu(II) configurations, and the four-fold coordinated Cu(II) centers are not tetrahedral, but square planar. This work also provides additional evidence that the hypervalent  $[\text{As}_4]^-$  centers play a role in photoinduced phenomena in both Cu-free arsenic chalcogenides, which is supported by the experimental observation [18] of a direct correlation of arsenic content with the magnitude of photodarkening in these materials, and Cu-containing arsenic chalcogenides.

S.I.S. is grateful to the EPSRC and Newton Trust for financial support. We thank the British Council and DAAD for provision of financial support.

---

\* Electronic address: sis24@cam.ac.uk

[1] K. S. Liang, A. Bienenstock, and C. W. Bates, Phys.

- Rev. B **10**, 1528 (1974).  
 [2] Z. M. Saleh, G. A. Williams, and P. C. Taylor, Phys. Rev. B **40**, 10557 (1989).  
 [3] G. J. Adriaenssens, A. G. de la Rocque, E. Belin-Ferré, and P. Hertogen, J. Non-Cryst. Solids **266-269**, 898 (2000).  
 [4] J. Z. Liu and P. C. Taylor, Phys. Rev. Lett. **59**, 1938 (1987).  
 [5] J. Z. Liu and P. C. Taylor, Phys. Rev. B **41**, 3163 (1990).  
 [6] N. Bollé, P. Hertogen, G. J. Adriaenssens, C. Sénémaud, and A. G. de la Rocque, Semiconductors **32**, 873 (1998).  
 [7] S. I. Simdyankin, T. A. Niehaus, G. Natarajan, T. Frauenheim, and S. R. Elliott, Phys. Rev. Lett. **94**, 086401 (2005).  
 [8] S. I. Simdyankin, S. R. Elliott, Z. Hajnal, T. A. Niehaus, and T. Frauenheim, Phys. Rev. B **69**, 144202 (2004).  
 [9] T. Frauenheim, G. Seifert, M. Elstner, T. Niehaus, C. Köhler, M. Amkreutz, M. Sternberg, Z. Hajnal, A. D. Carlo, and S. Suhai, J. Phys.: Condens. Matter **14**, 3015 (2002).  
 [10] D. Porezag, T. Frauenheim, T. Köhler, G. Seifert, and R. Kaschner, Phys. Rev. B **51**, 12947 (1995).  
 [11] M. Elstner, D. Porezag, G. Jungnickel, J. Elsner, M. Haugk, T. Frauenheim, S. Suhai, and G. Seifert, Phys. Rev. B **58**, 7260 (1998).  
 [12] T. Niehaus, M. Elstner, T. Frauenheim, and S. Suhai, J. Mol. Struct. THEOCHEM **541**, 185 (2001).  
 [13] T. A. Niehaus, unpublished.  
 [14] M. Elstner, unpublished.  
 [15] S. I. Simdyankin, S. R. Elliott, T. A. Niehaus, and T. Frauenheim, in “*Computational Modeling and Simulation of Materials III*”, edited by P. Vincenzini, A. Lami, and F. Zerbetto (Techna Group s.r.l., Faenza, Italy, 2004), vol. A, pp. 149–156.  
 [16] N. N. Greenwood and A. Earnshaw, *Chemistry of the Elements* (Butterworth/Heinemann, Oxford, 1997), 2nd ed.  
 [17] R. Atta-Fynn, P. Biswas, and D. A. Drabold, Phys. Rev. B **69**, 245204 (2004).  
 [18] A. Zakery, P. J. S. Ewen, and A. E. Owen, J. Non-Cryst. Solids **200**, 769 (1996).